ARTICLE

ACS chemical biology

Enhanced Antimicrobial Activity of Engineered Human Lysozyme

Thomas C. Scanlon[†], Charlotte C. Teneback[∥], Avinash Gill[†], Jenna L. Bement[∥], Joshua A. Weiner[‡], John W. Lamppa[†], Laurie W. Leclair[∥], and Karl E. Griswold[*,†,‡,§]

[†]Thayer School of Engineering, [‡]Program in Molecular and Cellular Biology, [§]Department of Biological Sciences, Dartmouth College, Hanover, New Hampshire 03755, and [∥]The Vermont Lung Center, Department of Medicine, University of Vermont College of Medicine, Burlington, Vermont 05405

ABSTRACT Lysozymes contain a disproportionately large fraction of cationic residues, and are thereby attracted toward the negatively charged surface of bacterial targets. Importantly, this conserved biophysical property may inhibit lysozyme antibacterial function during acute and chronic infections. A mouse model of acute pulmonary *Pseudomonas aeruginosa* infection demonstrated that anionic biopolymers accumulate to high concentrations in the infected lung, and the presence of these species correlates with decreased endogenous lysozyme activity. To develop antibacterial enzymes designed specifically to be used as antimicrobial agents in the infected airway, the electrostatic potential of human lysozyme (hLYS) was remodeled by protein engineering. A novel, high-throughput screen was implemented to functionally interrogate combinatorial libraries of charge-engineered hLYS proteins, and variants with improved bactericidal activity were isolated and characterized in detail. These studies illustrate a general mechanism by which polyanions inhibit lysozyme function, and they are the first direct demonstration that decreasing hLYS's net cationic character improves its antibacterial activity in the presence of disease-associated biopolymers. In addition to avoiding electrostatic sequestration, at least one charge-engineered variant also kills bacteria more rapidly in the absence of inhibitory biopolymers; this observation supports a novel hypothesis that tuning the cellular affinity of peptidoglycan hydrolases may be a general strategy for improving kinetics of bacterial killing.

Antibiotic resistance among bacterial pathogens represents a growing threat to public health. Of particular concern is the surprising rate at which resistance emerges under the selective pressure of conventional antibiotics (*1*), which typically function by inhibiting key cellular catalysts. Due in part to the abbreviated useful lifetime of new drugs, the number of new antibiotics approved by the Food and Drug Administration has been steadily declining for more than 20 years (*1*). The stagnation in research and development combined with widespread and sustained use of conventional therapeutic agents has driven the evolution and spread of resistance in pathogenic strains (*2*). Consequently, the physician's toolbox of efficacious antibacterial therapies has been steadily shrinking, and there is concern that multidrug-resistant and pan-resistant pathogens could soon represent widespread threats.

Human lysozyme (hLYS) is a particularly effective antimicrobial peptide (AMP) that catalytically hydrolyzes cell wall peptidoglycan (Figure 1) and has also been shown to exert catalysis-independent antimicrobial properties (*3*). These dual functions result in a protein that efficiently kills both Gram-positive and Gram-negative bacterial pathogens, and hLYS has been shown to be one of the most effective cationic AMPs in human airway fluids (*4, 5*). Lysozyme's catalytic mode of action represents a prospective advantage relative to conventional therapies. Conventional antibiotics and even antibody-based biotherapeutics act in a stoichiometric fashion, *i.e.*, each therapeutic molecule typically inhibits one target molecule in one cell. In contrast, a single hLYS enzyme has the capacity to rapidly hydrolyze thousands of glycosidic bonds and attack multiple bacterial cells. The catalytic nature of hLYS's antimicro-

*Corresponding author, karl.e.griswold@dartmouth.edu.

Received for review April 26, 2010 and accepted July 6, 2010.

Published online July 6, 2010

10.1021/cb1001119

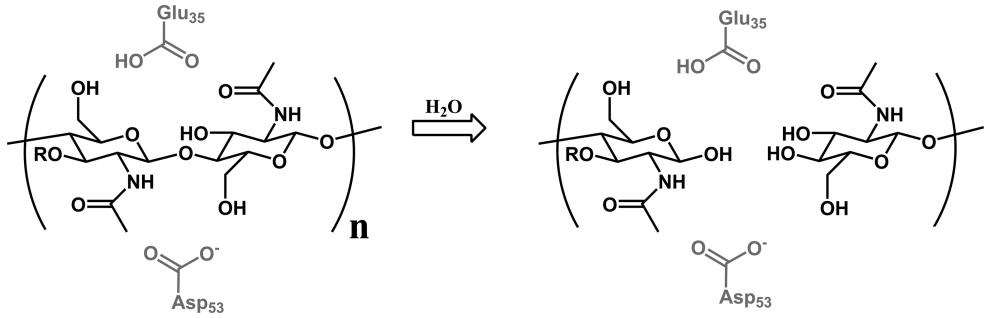

Figure 1. Lysozyme (hLYS) catalyzes hydrolysis of peptidoglycan. A line drawing representing the two repeating carbohydrate units of the bacterial cell wall: β(1→4)-linked *N*-acetyl muramic acid and *N*-acetyl glucosamine. The catalytic residues of hLYS are shown in gray. The "R" group of *N*-acetyl muramic acid represents a C2-ether linked lactic acid moiety that is in turn coupled to adjacent polysaccharide chains *via* short, cross-linking polypeptides. The resulting macromolecular net surrounds individual bacteria and forms the protective sacculus that opposes osmotic stress. Sacculus integrity and cell viability are compromised by hLYS-catalyzed hydrolysis of the polysaccharide chains.

bial activity may provide for lower dosing and superior efficacy.

Lysozymes are highly expressed in animal airways (*4, 5*) and have confirmed roles in combating infections (*6–8*). Yet bacterial infections of the animal airway are relatively common, suggesting that endogenous lysozyme function is diminished during acute or chronic infections. It is known that lower respiratory tract infections create a hyperinflammatory environment and result in local accumulation of densely charged anionic biopolymers. The concentrations of individual species such as F-actin, DNA, mucin, and the bacterial exopolysaccharide alginate can range from 100s of μg mL^{-1} to 10,000s of μg mL^{-1} in the infected lung (*9–11*). Unusually high concentrations of anionic biopolymers in the airway surface fluid can profoundly impact the local electrostatic environment and may ultimately compromise the efficacy of endogenous cationic AMPs. These observations have shaped a hypothesis that electrostatics drive complex formation between hLYS and anionic biopolymers (*12*) and that this sequestration is partially responsible for the apparent inability of hLYS to effect adequate bacterial clearance in lower respiratory tract infections. Complex formation between bacteriophage T4 lysozyme and negatively charged F-actin has been demonstrated *in vitro*, and a mutated variant of the T4 lysozyme having reduced net positive charge was shown to be less susceptible to electrostatic sequestration (*13*). Although the mutated enzyme was shown to maintain ~50% of the wild type enzyme's antibacterial activity in phosphate buffered saline, there was no analysis of bactericidal function in the presence of F-actin or other inhibitory biopolymers.

To develop highly active antimicrobial enzymes for prospective use in the infected lung, we sought to systematically remodel the electrostatic potential of hLYS. The conserved cationic nature of lysozymes indicates that at least some subset of charged residues is critical to the proteins' antibacterial function. Therefore, arbitrary mutation of charged residues was deemed unlikely to yield effective molecular designs. To more efficiently sample functional sequence space, we used multiple sequence alignments to identify those positively charged hLYS residues that are poorly conserved among other vertebrate lysozymes. We anticipated that some combination of these target residues might be mutated without disrupting bactericidal function. Combinatorial gene/protein libraries were constructed on the basis of our bioinformatics analysis, and subsequent functional screens yielded the first lysozymes specifically engineered for enhanced antibacterial activity in the infected airway.

RESULTS AND DISCUSSION

Anionic Biopolymers Inhibit Wild Type Lysozyme Function. The positive charge of cationic AMPs, including hLYS, guides these natural antibiotics to their targets and is one key means by which AMPs manifest specificity for bacteria (*14*). In cases of acute and chronic lung infection, however, electrostatic sequestration with anionic biopolymers may contribute to a generalized, systematic inactivation of cationic AMPs. We used a mouse

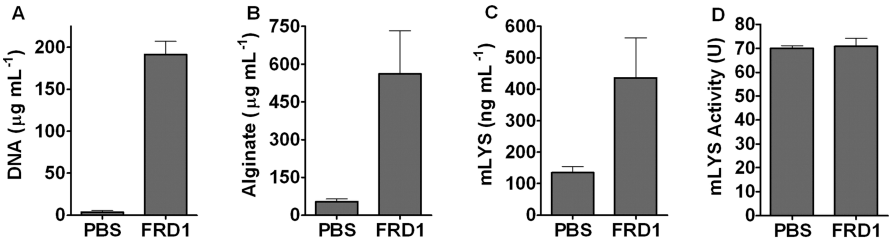

Figure 2. Analysis of anionic biopolymers and lysozyme activity in a murine model of pulmonary infection. Mucoid *P. aeruginosa* strain FRD1 or a PBS control was administered to the airways of C57Bl/6 mice, and bronchoalveolar lavage (BAL) fluid was collected 24 h postinfection. A) High concentrations of dsDNA were observed in cell-free BAL from *P. aeruginosa* infected mice compared to control mice, which had no detectable extracellular DNA. B) Cell-free BAL fluid was analyzed for alginate content using a novel enzymatic method. The assay showed BAL fluid from infected mice contained more than 500 μg mL^{-1} of alginate, whereas BAL fluid from noninfected mice produced a signal only marginally above background. C) A 3.2-fold increase in mouse lysozyme was observed in infected mice, compared to PBS-treated animals. D) Cell-free BAL was assayed for endogenous mouse lysozyme activity by kinetic microplate assay, as described in the text. Although lysozyme protein levels were significantly elevated following infection, lysozyme activity levels were virtually identical in the infected and control groups. Error bars represent the SEM in all panels.

model of acute *Pseudomonas aeruginosa* pulmonary infection to explore the biological relevance of polyanion accumulation in pulmonary infections and to examine possible correlated effects on endogenous lysozyme function. The airways of C57BL/6 mice were infected *via* oropharyngeal aspiration of ~10^7 colony forming units (cfu) of *P. aeruginosa* strain FRD1, a mucoid clinical isolate. Twenty-four hours postinfection, alginate and extracellular DNA levels were analyzed in bronchoalveolar lavage (BAL) fluid from both groups. Extracellular DNA was not detectable in the BAL fluid of control mice but exceeded 190 μg mL^{-1} in BAL fluid from the infected group (Figure 2, panel A). Similarly, we observed a 10-fold higher concentration of alginate exopolysaccharide in the BAL fluid of infected mice (Figure 2, panel B). To monitor alginate in BAL samples, we used an enzymatic assay employing purified bacterial alginate lyase. The enzyme specifically degrades alginate and produces a reaction product that can be detected spectrophotometrically (*15*). Alginate in experimental BAL samples is quantified by interpolation using standard curves produced with purified bacterial alginate. We speculate that enzymatic detection of alginate in BAL samples represents a significant advance over standard morphology-based mucoid phenotype detection on agar plates. In particular, our assay directly quantifies alginate in diagnostic samples and may enable detection of transient alginate producing phenotypes that revert to a nonmucoid morphology when cultured outside of the infected lung.

Consistent with an immune response to acute infection, ELISA assays of BAL fluid show that the airway surface liquid of infected mice contained 3.2-fold more endogenous mouse lysozyme protein than comparable control samples (Figure 2, panel C). The BAL fluid of infected and control groups, however, exhibited equivalent levels of lysozyme enzymatic activity (Figure 2, panel D). In aggregate, these observations demonstrate that pulmonary infection with *P. aeruginosa* causes elevated concentrations of extracellular, anionic biopolymers in the lung, and the appearance of these species correlates with reduced endogenous lysozyme activity. Importantly, the values reported in Figure 2 are those in the BAL fluid and not the airway surface liquid itself. The considerable dilution resulting from the lavage process implies that the *in vivo* concentrations of extracellular DNA and alginate are likely much greater.

To probe whether the human enzyme was subject to similar inhibitory mechanisms, recombinant hLYS was analyzed by *in vitro* kinetic assays in the presence of high molecular weight DNA, alginate, and mucin. All 3 polyanions showed a dose−response effect, with complete inhibition of wild type hLYS between 1 and 5 mg mL^{-1} polyanion (Figure 3). Thus, lysozymes appear to be particularly susceptible to inactivation by molecules that are elevated in the infected and inflamed airway.

Design and Construction of Charge-Engineered hLYS Libraries. We speculated that the observed *in vitro* and *in vivo* inhibition of lysozyme stemmed from electrostatic mediated sequestration. Previous studies have shown that T4 phage lysozyme forms electrostatic complexes with F-actin *in vitro* and that charge modification of the enzyme can reduce the extent of these electro-

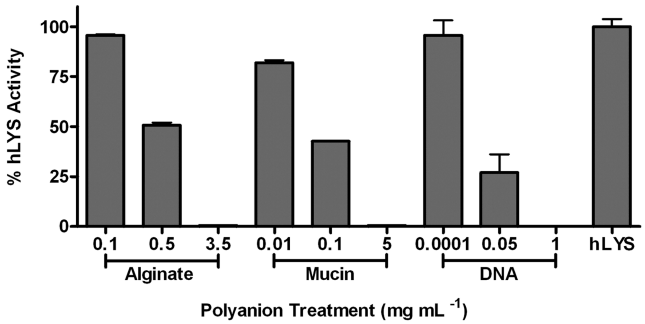

Figure 3. Alginate, mucin, and DNA inhibit hLYS-mediated lysis of *M. luteus* in a dose−response fashion, and each causes complete inhibition at physiologically relevant concentrations. Activities were normalized to that of hLYS in the absence of inhibitory biopolymers (hLYS). Error bars represent the SEM.

static interactions (*13*). These pioneering studies represent a key conceptual demonstration, but the clinical utility of the enzymes described in ref 13 is less clear. Specifically, the viral origin of T4 lysozyme could prompt a detrimental immune response in human patients, and moreover there was no direct demonstration of the modified T4 lysozyme's antibacterial activity in the presence of F-actin or other anionic biopolymers. We therefore aimed to build upon this prior work and develop antibacterial enzymes with greater clinical potential. To this end, we specified that our molecular designs should have bactericidal activity *in the presence of disease associated polyanions*, and we employed a human enzyme scaffold in order to mitigate the intrinsic immunogenicity of nonhuman proteins (*16*).

The hLYS crystal structure 1LZS (chain A) was compared against a panel of 50 structural homologues using the ConSurf web server (*17*). The analysis produced position-specific evolutionary conservation scores for the hLYS template. Assuming that highly conserved residues are likely essential for hLYS function, eight basic residues with the lowest conservation scores (*i.e.*, color scores ≤ 4) were selected for mutagenesis (R14, R21, R41, R50, H78, R101, R115, and R122). Two gene libraries were constructed as described previously (*18*). The first was designated the "NDA Library", in which target sites encoded wild-type, Asn, Asp, or Ala residues, and the second the "QEA Library" encoding wild-type, Gln, Glu, or Ala residues. The alpha mating factor signal peptide directed enzyme secretion from yeast, and the libraries were subjected to high-throughput functional screening as described below. After selection and characterization of first generation clones, a second generation "shuffled" library was constructed using the 22 mutations associated with the highest activity NDA and QEA enzymes.

High-Throughput Functional Screening. To rapidly screen yeast libraries for lytic activity, solid yeast growth media was supplemented with UV-inactivated, freeze-dried *Micrococcus luteus* reporter bacteria at concentrations sufficient to cause bulk phase turbidity. Yeast colonies secreting wild type hLYS lyse the underlying *M. luteus* cells, forming visible zones of clearance. Incorporating alginate in the screening media inhibits the lytic activity of the wild type enzyme (Figure 4). It was anticipated that mutating cationic residues would improve hLYS's diffusivity in alginate hydrogels and that a subset of these aggregation-resistant variants would retain catalytic function and restore the halo-forming phenotype of the corresponding colonies. Thus, our agarose plate assay provides a method to simultaneously evaluate catalytic activity and diffusivity in polyanion hydrogels.

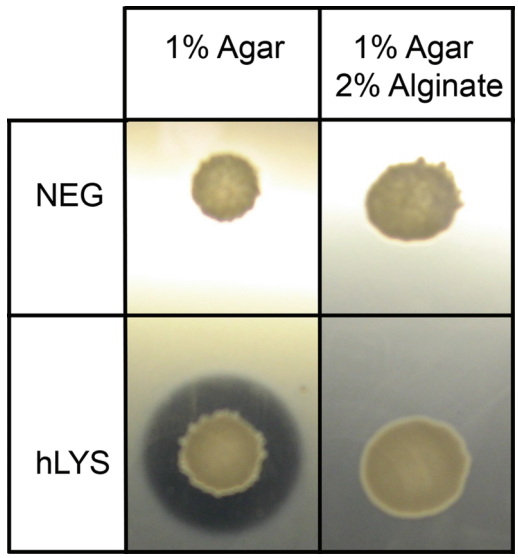

Figure 4. Plate-based halo formation screen for enhanced hLYS activity. In the absence of alginate inhibitor, yeast secreting wild type hLYS generate a zone of clearance due to *M. luteus* lysis (lower left panel), whereas yeast secreting a scrambled peptide do not (upper left panel). Yeast secreting wild type hLYS fail to generate a zone of clearance on media containing alginate inhibitor (lower right panel).

The NDA and QEA libraries were functionally interrogated using alginate (1.75% w/v) screening media, and the populations were oversampled so as to yield 99.95% theoretical coverage (*19*). The NDA library yielded 18 validated clones (~0.004% hit rate based on total clones screened), and the QEA library yielded 51 (~0.01% hit rate). Validated first generation clones were sequenced, and a "shuffled" second generation library was constructed by incorporation of synthetic oligonucleotides by gene reassembly (ISOR) using synthetic oligonucleotides encoding each mutation found in selected first generation variants. Due to the presumed enhanced functionality of second generation library members, subsequent screening employed increased stringency, *i.e.*, 3% (w/v) alginate media. Approximately 175,000 second generation clones were interrogated, providing >99.99% coverage of the theoretical 16,875 member library. Despite the increased screening stringency, the second generation library produced a substantially higher hit rate (176 clones, 0.10%). Interestingly, all selected second generation clones bore an R115H mutation that was observed in one first generation NDA clone. As this was not one of the designed mutations, its original source was likely an oligonucleotide impurity in the NDA library. Importantly, 20 randomly selected clones, sequenced before screening, showed no bias for the R115H mutation. Thus, its dominance in the second generation clones highlights the mutation's functional significance.

A semiquantitative, fluorogenic, 96-well plate assay was developed to rank-order the lytic activity of selected enzyme variants. The SyTox Green nucleic acid stain is largely impermeant to UV-inactivated and lyophilized *M. luteus* bacterial cells despite their nonviable state. Addition of active lysozyme to *M. luteus*−SyTox mixtures produces a fluorescent signal as cell walls are degraded and SyTox dye intercalates into exposed genomic DNA. The activity of culture supernatant from selected clones was assessed by the fluorogenic cell wall permeability assay, and the results were compared to a wild type hLYS control. Kinetic data were acquired in both the presence and absence of inhibitory alginate biopolymer, and maximum slopes were normalized to enzyme concentrations based on densitometry of Coomassie stained SDS-PAGE gels. A total of 102 variants were assessed for specific activity in the presence and absence of alginate. All engineered enzymes possessed dramatically improved kinetics in the presence of 1.0% (w/v) alginate (Figure 5, *y*-axis), which is sufficient to completely inhibit the wild type enzyme. Under noninhibitory conditions, however, the majority of charge modified variants exhibited reduced enzyme activity (Figure 5, *x*-axis). These results demonstrate that charge-reducing mutations generally compromise inherent hLYS activity but rare amino acid substitutions can produce variants with superior all-around performance (e.g., 2-3-7, upper right quadrant of Figure 5). Ultimately, five enzyme variants having high levels of activity both in the presence and absence of alginate were selected for more detailed characterization.

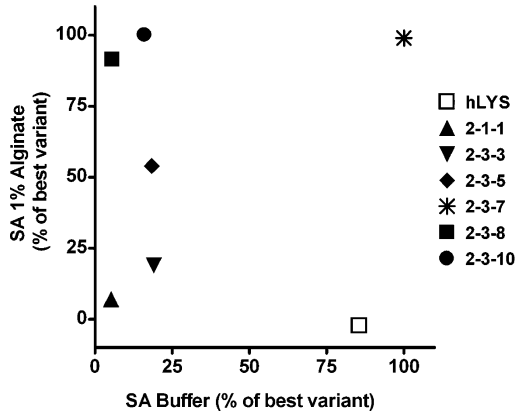

Figure 5. Secondary screen for charge-engineered hLYS variants. Charge-engineered hLYS variants secreted from induced cultures of recombinant *S. cerevisiae* were tested for enzyme activity using the fluorogenic membrane permeability assay in the absence or presence of polyanion inhibitor. Specific activity (SA) measurements in buffer alone (*x*-axis) were plotted against specific activity in the presence of 1% (w/v) alginate (*y*-axis). Data from six representative variants and the wild type enzyme are shown. Specific activities are presented as a percentage of the most active enzyme in each condition. Charge-engineered variants displaying high relative activity in the absence and presence of alginate (e.g., variant 2-3-7) were selected for further characterization.

Gram-Negative Bactericidal Activity. Because the high-throughput halo screen assessed lytic activity against Gram-positive bacteria, it was not known *a priori* whether the engineered enzymes would also kill Gram-negative pathogens. This latter function is particularly relevant to clinical applications, as Gram-negative infections are becoming increasingly difficult to treat (*20*). To assess this important metric of prospective clinical utility, the five most promising hLYS variants were

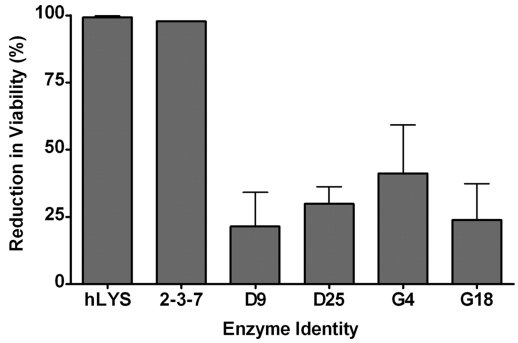

Figure 6. Bactericidal activity toward Gram-negative *P. aeruginosa*. Purified enzymes (75 μg mL^{-1}) were incubated with *P. aeruginosa* strain PAO1 (25,000 cfu mL^{-1}) for 30 min, and viability was quantified by plating serial dilutions and enumerating cfu's upon overnight outgrowth. Results were normalized to a buffer control treatment, *i.e.*, no reduction in viability. Only variant 2-3-7 retained high level anti-pseudomonal activity comparable to wild type hLYS. Error bars represent the SEM.

purified by cation exchange chromatography and tested for anti-pseudomonal activity by standard quantitative culture assays. Only variant 2-3-7 exhibited high-level bactericidal activity toward *P. aeruginosa* (98.5% that of wild type hLYS activity; Figure 6). Given the high-throughput screen's readout of catalytic antimicrobial activity and the fact that Gram-negative lysozyme activity is thought to occur by a catalysis-independent mechanism (*3*), these results were not entirely surprising. Because of its capacity to attack both Gram-positive and Gram-negative bacterial targets, variant 2-3-7 was the focus of subsequent studies.

Kinetic Characterization of hLYS Variant 2-3-7. Prompted by promising preliminary results, the catalytic properties of variant 2-3-7 were analyzed in greater detail. Pseudo Michaelis–Menten analyses of 2-3-7 and wild type hLYS were performed using conventional light scattering assays with freeze-dried *M. luteus* as a substrate. Although the insoluble nature of the cellular substrate and the complexity of the catalysis–lysis relationship preclude direct mechanistic interpretation of the calculated kinetic parameters, the results are suitable for comparison of relative enzyme performance. In the absence of biopolymer inhibitors, the apparent K_m of wild type hLYS was 100 μg mL^{-1} and its V_{max} was 900 $\Delta A_{450\ nm}$ min^{-1} mg^{-1}. These results are largely consistent with previous kinetic analysis of hLYS (*21*). In comparison, variant 2-3-7 possessed an apparent K_m of 40 μg mL^{-1} and a V_{max} of 720 $\Delta A_{450\ nm}$ min^{-1} mg^{-1}. Thus, the two enzymes are essentially equally active in the absence of inhibitor, with 2-3-7 exhibiting perhaps a slight advantage in efficiency (V_{max}/K_m).

In contrast, the enhanced performance of 2-3-7 in the presence of polyanion inhibitors was striking. The specific activities of both enzymes were evaluated over several log dilutions of physiologically relevant anionic biopolymers, and IC_{50} values were determined by fitting the data to sigmoidal dose–response curves. Compared to wild type hLYS, the IC_{50} values of variant 2-3-7 were 3-fold higher with alginate, 7-fold higher with mucin, and an impressive 43-fold higher with double stranded DNA (Table 1). Importantly, the high-throughput library screen for enzyme function was based on alginate as the sole inhibitor. Therefore, the enhanced functionality of 2-3-7 with a broader array of anionic biopolymers underscores the nonspecific nature of electrostatically mediated lysozyme inhibition. By demonstrating increases in IC_{50} to a panel of structurally distinct anionic biopolymers, we experimentally validate charge engineering as an approach for developing novel, functional cationic AMP therapies active in the presence of diverse and physiologically relevant anionic biopolymers.

During the process of enzyme characterization, two different kinetic assays had been employed: conventional light scattering (*22*) and a fluorogenic cell wall permeability assay. The need for the fluorogenic assay stemmed in part from the fact that concentrated mucin

TABLE 1. Kinetics and IC_{50} values for hLYS and variant 2-3-7; pseudo Michaelis–Menten parameters are reported ± SEM

Enzyme	V_{max} (ΔA_{450} [min mg]$^{-1}$)	K_m^{App} (μg mL^{-1})	V_{max}/K_m^{App}	IC_{50} alginate (μg mL^{-1})	IC_{50} mucin (μg mL^{-1})	IC_{50} DNA (μg mL^{-1})
hLYS	900 ± 100	100 ± 30	9	370	105	31
2-3-7	720 ± 50	40 ± 10	18	1150	730	1336

and alginate solutions are inherently turbid and interfere with signal detection by light scattering. In the absence of any inhibitory biopolymer the two assays yielded unexpectedly different results. Light scattering assays showed that, in the absence of inhibitor and at high substrate concentrations, wild type hLYS and variant 2-3-7 exhibited roughly equivalent lytic rates (Figure 7, panel A). In contrast, the fluorogenic assay performed under identical conditions showed that 2-3-7 was 300% faster (Figure 7, panel B). This apparent discrepancy highlights a mechanistic distinction between the two analytical techniques. Signal detection by light scattering requires full lysis of target bacteria. In contrast, detection with the SyTox fluorogenic assay requires only sufficient peptidoglycan hydrolysis to disrupt the cell wall's function as a barrier to diffusion. With respect to therapeutic applications, it is almost certain that sublytic cell wall damage is sufficient for killing. Therefore the novel use of SyTox dye for lysozyme kinetic analysis may provide a more clinically relevant metric than conventional light scattering measurements.

It is commonly assumed that lysozyme's exceptionally dense positive charge is critical to its antibiotic function (*23*). This prevailing view has been supported by previous mutagenesis studies in which reduction of hLYS's positive charge resulted in decreased lytic activity under all conditions except the lowest ionic strengths (*24*). Additionally, at least one group has attempted to improve lysozyme's antibacterial properties by conjugation to highly cationic nanoparticles (*25*). Our results question previous assumptions regarding the relationship between lysozyme charge and antibacterial function. In particular, we emphasize that lysozyme-mediated bacterial death does not require complete lysis but instead occurs when diffusional barriers to the cell's cytoplasm are compromised. Under the conditions tested here, the charge density of wild type hLYS appears to drive excessively strong association with bacteria and results in processive-like peptidoglycan hydrolysis beyond the point at which bacterial death occurs. As a result, the wild type enzyme rapidly degrades a subset of bacterial targets to the point of lysis, but is slower to act upon bacterial populations as a whole. Conversely, the reduced charge of 2-3-7 (Δ-3 from hLYS) likely results in faster off rates from bacterial surfaces, and as a consequence, 2-3-7 would be expected to more rapidly establish a homogeneous distribution in concentrated cell suspensions. Accordingly, the engineered enzyme would effect damage to a greater number of target cells. This hypothesis explains the variant's enhanced kinetics in the fluorogenic assay and also suggests that the corresponding kinetics of actual bacterial killing should be improved.

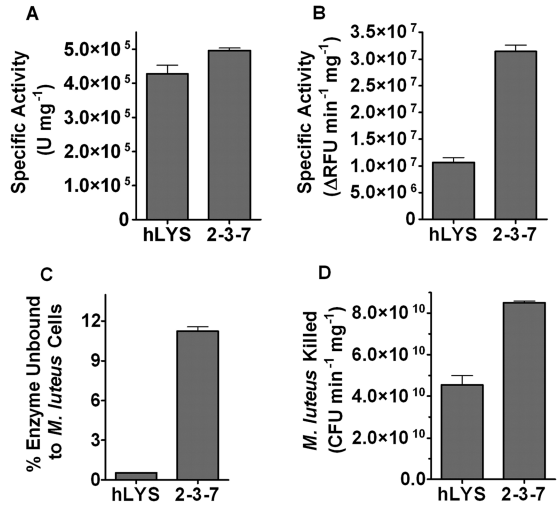

Figure 7. Charge engineering improves noninhibited hLYS kinetics. A) In the absence of inhibitor, specific activities of wild type hLYS and variant 2-3-7 are highly similar ($p = 0.167$) as assessed by light scattering of *M. luteus* bacteria at 750 μg mL^{-1}. Importantly, signal detection requires lysis of target cells. B) Under identical reaction conditions, a fluorogenic cell wall permeability assay reveals that 2-3-7 damages cell walls 300% faster than hLYS. In contrast to light scattering, sublytic peptidoglycan degradation is sufficient for detection with the fluorogenic SyTox Green probe. C) Cell wall binding was assessed by brief incubation of each enzyme with *M. luteus* suspensions and subsequent separation of bacteria by centrifugation. Data are presented as percentage of initial enzyme activity remaining in the supernatant, *i.e.*, unbound enzyme. More than 11% of variant 2-3-7 was found in the supernatant, whereas less than 1% of hLYS remained unbound. D) The kinetics of *M. luteus* killing by each enzyme were assessed by time course quantitative culture. Specific rates of killing were determined by linear regression of cfu *versus* time data. Under identical conditions, variant 2-3-7 kills *M. luteus* cells approximately 2-fold faster than hLYS. Error bars represent SEM.

To experimentally confirm the reduced affinity of 2-3-7 for bacterial surfaces, enzyme−bacteria pull down experiments were performed. The variant and wild type enzymes were mixed with *M. luteus* cells for <5 s, and unbound enzyme was separated from the bacterial cells by brief high speed centrifugation and careful removal of supernatant. It was observed that >99% of wild type hLYS was associated with the bacterial pellet, whereas more than 11% of 2-3-7 remained in solution (Figure 7, panel C).

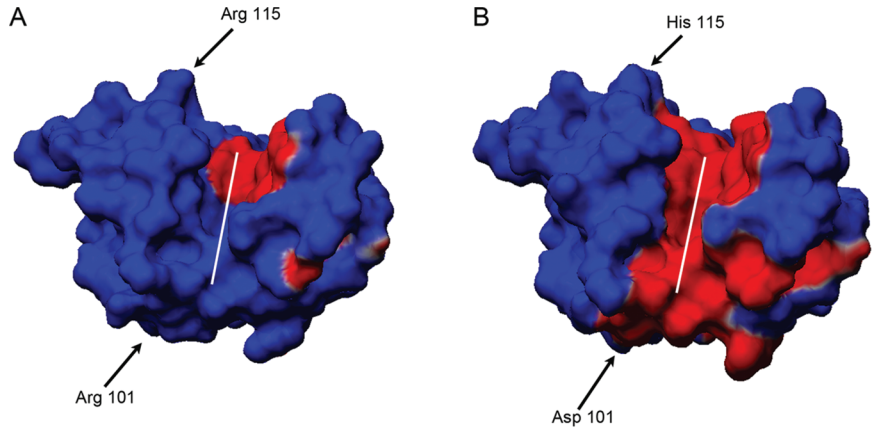

Figure 8. Two mutations radically alter electrostatic surface potential of hLYS. Relative electrostatic potentials mapped to the molecular surfaces of (A) wild type hLYS (PDB code 1JWR) and (B) variant 2-3-7 (PDB code 3LN2). Positive potential is blue, and negative potential is red. The white lines indicate the approximate location of the active site cleft, and the positions of the two mutated residues are noted with arrows. The two mutations resulted in little alteration to the global enzyme structure (overall superposition of the two structures yielded an rmsd = 0.97) but dramatically reshaped the electrostatic potential of 2-3-7 as shown by the considerable expansion of negative surface potential. A movie showing the entirety of both protein surfaces is provided in Supporting Information.

To determine whether the charge-engineered variant would indeed exhibit an enhanced rate of killing, kinetic viability experiments were performed with both wild type hLYS and 2-3-7. Consistent with our hypothesis, these experiments demonstrated that the engineered enzyme exhibited approximately 2-fold faster specific rates of killing compared with wild type hLYS (Figure 7, panel D). The reduced charge of 2-3-7 is thought to facilitate faster dissociation from the surface of bacteria, action upon a greater total number of target cells, and ultimately enhanced lethality in dense bacterial suspensions. Thus, mutations that site-specifically reduce hLYS's cationic character can enhance bactericidal capacity irrespective of the presence or absence of inhibitory polyanions.

The findings of this study suggest that modulating affinity for bacterial targets could represent a general method for improving the biocidal activity of lytic enzymes. Cell wall hydrolases from numerous sources are currently considered attractive antibacterial candidates (*26*). While evolution has optimized the catalytic domains of these enzymes for potent lytic activity, their molecular properties, in aggregate, may not be ideal for therapeutic applications. Indeed, phage lysins employ potent cell wall binding domains, and it has been suggested that they represent "single-use" enzymes that bind cell wall targets with near irreversibility (*27*). Because each molecule may act upon a single cellular target, relatively high dosing of phage lysins might be required to effectively treat an infection. The studies described here suggest a previously unrecognized paradigm for engineering cell wall hydrolases as antibacterial therapies: tuning cell wall affinity enhances overall bactericidal function.

Molecular Origin of Enhanced Activity. At a pH of 7.0, wild type hLYS (pI = 9.28) has a calculated net charge of +7.77, whereas variant 2-3-7 (pI = 8.85) has a net charge of only +4.86. While this considerable change in global charge state explains the enhanced performance of 2-3-7 in a very general sense, the precise spatial distribution of a protein's charge is more relevant to its function and interaction with other charged species. To visualize the effects of 2-3-7's mutations in finer detail, the electrostatic potential surfaces of wild type hLYS (PDB code 1JWR) and variant 2-3-7 (PDB code 3LN2) were calculated using identical parameters. Only three regions of negative potential were observed on the wild type hLYS surface, the most substantial of which was proximal to the catalytic residues Asp53 and Glu35 (Figure 8, panel A). As discussed above, the wild type protein's overwhelming positive potential drives electrostatic complex formation with negatively charged biopolymers. In contrast, the mutations R101D and R115H radically reshape the potential surface of variant 2-3-7 (Figure 8, panel B). The negative potential of the charge modified variant spans the entire active site cleft and extends in a continuous fashion to the distal

side of the protein (see Supplementary Movie File). Importantly, a superposition of the 1JWR and 3LN2 crystal structures showed little deviation (rmsd = 0.37 for backbone atoms and rmsd = 0.97 overall), indicating that the differences in the calculated potentials result primarily from the charge-altering mutations as opposed to gross structural reorganization. It appears that certain regions of dense positive surface potential are in fact important for hLYS function but that the electrostatics of the active site cleft can be remodeled while maintaining antibacterial efficacy.

In summary, the overall enhanced functionality of 2-3-7 suggests that appropriately reducing positive charge may be a powerful strategy for enhancing lysozyme function in the infected lung environment and beyond. Looking to the future, hLYS may represent an adaptable scaffold upon which diverse panels of highly efficacious, biocatalytic antibiotics can be engineered.

METHODS

Strains and Plasmids. *S. cerevisiae* expression host BJ5464 (*28*) and *M. luteus* bacteria were obtained from ATCC. *P. aeruginosa* strains PAO1 and FRD1 were gifts from George O'Toole (Dartmouth College). Propagation of plasmids was performed in *E. coli* DH5α. Construction of the centromeric expression vector p4GM-LYZ has been described previously (*18*).

Mouse Model of *P. aeruginosa* Infection. Overnight cultures of *P. aeruginosa* FRD1 clones grown in LB were pelleted, washed, and resuspended in PBS to a concentration of approximately 10^7 cfu per 40 μL. C57BL/6 male mice were briefly anesthetized with isoflourane and inoculated by oropharyngeal aspiration (*29*). After 24 h, mice were anesthetized with IP pentobarbital (90 mg kg^{-1}), the trachea was cannulated, and the lung lavaged with 1 mL of PBS. BAL fluid was centrifuged at 1600 rpm for 5 min to remove airway cells and used for follow on studies. All animal protocols were approved by the University of Vermont Institutional Animal Care and Use Committee, and procedures were performed according to their guidelines.

Quantifying Polyanions of the Mouse Lung. Measurements for extracellular dsDNA in cell-free BAL from infected/control mice were performed using a fluorescence assay. Fluorescence intensity of 250 μL samples of cell-free BAL mixed with 50 nM SyTox Green was measured in microplate format and compared to a serial dilution of salmon sperm DNA (Figure 2, panel A). Kinetic measurement of alginate lyase enzyme activity was used to determine alginate concentration in cell-free BAL fluid from infected/control mice. To remove interfering DNA, BAL was prepared as previously described (*30*). A 195 μL sample of prepared BAL was mixed with 250 ng of purified A1-III alginate lyase in UV-transparent 96-well plates; kinetic measurements of absorbance at 235 nm were recorded, and initial rates were compared to a standard curve of A1-III activity against known concentrations of purified FRD1 alginate (Figure 2, panel B).

Analysis of Airway Mouse Lysozyme Expression/Activity. Cell-free BAL from mice infected with FRD1 was assayed for endogenous lysozyme using a Mouse Lysozyme ELISA Kit (CUSABIO Biotech Co.) according to manufacturer's recommendations (Figure 2, panel C). Lytic activity of endogenous lysozyme (Figure 2, panel D) was measured as described in Supporting Information.

hLYS Activity Measurements. Light scattering assays were performed essentially as described by Lee and Yang (*22*). Reaction conditions for the fluorogenic membrane permeability assay can be found in Supporting Information.

Construction of Mutant Libraries. Sequences for synthetic oligonucleotides were designed for mutagenesis of 8 hLYS residues (R14, R21, R41, R50, H78, R101, R115, and R122) and are reported in Supplementary Table 1. Following ISOR (*31*), mutagenic amplicons and appropriately restricted expression vector were electroporated into freshly prepared yeast expression host exactly as described in ref 18. Typical transformation efficiency was 1.0×10^7 cfu μg^{-1} backbone vector.

Functional Screening of Libraries. Recombinant yeast expressing charge-engineered hLYS variants were subjected to high-throughput screening on alginate screening media. Details of yeast plating and screening can be found in Supporting Information.

Anti-pseudomonal Activity. For anti-pseudomonal assays, 25,000 cfu mL^{-1} of midlog cultures of *P. aeruginosa* strain PAO1 were mixed with 7.5 μg of purified hLYS variants in activity buffer (10% LB v/v, 10 mM potassium phosphate, pH 7.0) in a total reaction volume of 115 μL. Mutant hLYS enzymes were purified as described in Supporting Information. Dilutions were plated after a 60 min incubation at 37 °C, colonies were enumerated after overnight outgrowth, and results were compared to dilution plates sampled at time zero (Figure 6).

***M. luteus* Binding and Viability Experiments.** For hLYS−*M. luteus* binding experiments, 800 ng mL^{-1} hLYS variant was mixed with 750 μg mL^{-1} *M. luteus*, and unbound enzyme was quantified as described in Supporting Information. Data are represented as percent of unbound enzyme (Figure 7, panel C). For viability experiments, *M. luteus* (final $OD_{600\ nm}$ 0.75) was mixed with 50 ng hLYS enzymes in 200 μL reactions and incubated for several minutes. Reactions were sampled at various time points, and remaining viable bacteria were assessed by microplate dilution and quantitative culture. Values are represented as change in viable *M. luteus* cfu per minute per microgram enzyme (Figure 7, panel D) as described in Supporting Information.

Calculation of Electrostatic Potentials. The electrostatic potential surfaces of wild type hLYS (PDB code 1JWR) and variant 2-3-7 (PDB code 3LN2) were calculated using the Yasara Structure software suite (*32*). Details are included in Supporting Information.

Acknowledgment: This work was supported by a Wallace H. Coulter Foundation Early Career Award, a Cystic Fibrosis Foundation Carol Basbaum Memorial Postdoctoral Fellowship (SCANLO08F0), and P20RR018787-06 from the National Center for Research Resources (NCRR), a component of the NIH. The authors thank M. Wargo for assistance with mouse studies, and G. O'Toole and T. Gerngross for critical comments on the manuscript.

K.E.G. and T.C.S. have filed a patent application for therapeutic use of charge-engineered human lysozyme variants.

Supporting Information Available: This material is available free of charge *via* the Internet at http://pubs.acs.org.

REFERENCES

1. Taubes, G. (2008) The bacteria fight back, *Science (New York, NY) 321*, 356–361.

2. Furuya, E. Y., and Lowy, F. D. (2006) Antimicrobial-resistant bacteria in the community setting, *Nat. Rev. Microbiol. 4*, 36–45.
3. Nash, J. A., Ballard, T. N. S., Weaver, T. E., and Akinbi, H. T. (2006) The peptidoglycan-degrading property of lysozyme is not required for bactericidal activity in vivo, *J. Immunol. 177*, 519–526.
4. Cole, A. M., Liao, H.-I., Stuchlik, O., Tilan, J., Pohl, J., and Ganz, T. (2002) Cationic polypeptides are required for antibacterial activity of human airway fluid, *J. Immunol. 169*, 6985–6991.
5. Travis, S. M., Conway, B. A. D., Zabner, J., Smith, J. J., Anderson, N. N., Singh, P. K., Greenberg, E. P., and Welsh, M. J. (1999) Activity of abundant antimicrobials of the human airway, *Am. J. Respir. Cell Mol. Biol. 20*, 872–879.
6. Akinbi, H. T., Epaud, R., Bhatt, H., and Weaver, T. E. (2000) Bacterial killing is enhanced by expression of lysozyme in the lungs of transgenic mice, *J. Immunol. 165*, 5760–5766.
7. Cole, A. M., Thapa, D. R., Gabayan, V., Liao, H.-I., Liu, L., and Ganz, T. (2005) Decreased clearance of *Pseudomonas aeruginosa* from airways of mice deficient in lysozyme M, *J. Leukocyte Biol. 78*, 1081–1085.
8. Dajani, R., Zhang, Y., Taft, P. J., Travis, S. M., Starner, T. D., Olsen, A., Zabner, J., Welsh, M. J., and Engelhardt, J. F. (2005) Lysozyme secretion by submucosal glands protects the airway from bacterial infection, *Am. J. Respir. Cell Mol. Biol. 32*, 548–552.
9. Ramsey, D. M., and Wozniak, D. J. (2005) Understanding the control of *Pseudomonas aeruginosa* alginate synthesis and the prospects for management of chronic infections in cystic fibrosis, *Mol. Microbiol. 56*, 309–322.
10. Rogers, D. F. (2007) Physiology of airway mucus secretion and pathophysiology of hypersecretion, *Respir. Care 52*, 1134–1149.
11. Ulmer, J. S., Herzka, A., Toy, K. J., Baker, D. L., Dodge, A. H., Sinicropi, D., Shak, S., and Lazarus, R. A. (1996) Engineering actin-resistant human DNase I for treatment of cystic fibrosis, *Proc. Natl. Acad. Sci. U.S.A. 93*, 8225–8229.
12. Weiner, D. J., Bucki, R., and Janmey, P. A. (2003) The antimicrobial activity of the cathelicidin LL37 is inhibited by F-actin bundles and restored by gelsolin, *Am. J. Respir. Cell Mol. Biol. 28*, 738–745.
13. Sanders, L. K., Xian, W., Guaqueta, C., Strohman, M. J., Vrasich, C. R., Luijten, E., and Wong, G. C. L. (2007) Control of electrostatic interactions between F-actin and genetically modified lysozyme in aqueous media, *Proc. Natl. Acad. Sci. U.S.A. 104*, 15994–15999.
14. Matsuzaki, K. (2009) Control of cell selectivity of antimicrobial peptides, *Biochim. Biophys. Acta, Biomembr. 1788*, 1687–1692.
15. Preiss, J., and Ashwell, G. (1962) Alginic acid metabolism in bacteria. I. Enzymatic formation of unsaturated oligosac-charides and 4-deoxy-L-erythro-5-hexoseulose uronic acid, *J. Biol. Chem. 237*, 309–316.
16. Schellekens, H. (2005) Factors influencing the immunogenicity of therapeutic proteins, *Nephrol., Dial., Transplant. 20*, vi3–9.
17. Landau, M., Mayrose, I., Rosenberg, Y., Glaser, F., Martz, E., Pupko, T., and Ben-Tal, N. (2005) ConSurf 2005: the projection of evolutionary conservation scores of residues on protein structures, *Nucleic Acids Res. 33*, W299–302.
18. Scanlon, T., Gray, E., and Griswold, K. (2009) Quantifying and resolving multiple vector transformants in *S. cerevisiae* plasmid libraries, *BMC Biotechnol. 9*, 95.
19. Patrick, W. M., Firth, A. E., and Blackburn, J. M. (2003) User-friendly algorithms for estimating completeness and diversity in randomized protein-encoding libraries, *Protein Eng. 16*, 451–457.
20. Livermore, D. M. (2009) Has the era of untreatable infections arrived? *J. Antimicrob. Chemother. 64*, i29–36.
21. Muraki, M., Harata, K., Sugita, N., and Sato, K. (2000) Protein-carbohydrate interactions in human lysozyme probed by combining site-directed mutagenesis and affinity labeling, *Biochemistry 39*, 292–299.
22. Lee, Y. C., and Yang, D. (2002) Determination of lysozyme activities in a microplate format, *Anal. Biochem. 310*, 223–224.
23. Price, J. A., and Pethig, R. (1986) Surface charge measurements on *Micrococcus lysodeikticus* and the catalytic implications for lysozyme, *Biochim. Biophys. Acta 889*, 128–135.
24. Muraki, M., Morikawa, M., Jigami, Y., and Tanaka, H. (1988) Engineering of human lysozyme as a polyelectrolyte by the alternation of molecular surface charge, *Protein Eng. 2*, 49–54.
25. Rohan, S., and Alexey, V. (2008) Charge-directed targeting of antimicrobial protein-nanoparticle conjugates, *Biotechnol. Bioeng. 100*, 403–412.
26. Donovan, D. M. (2007) Bacteriophage and peptidoglycan degrading enzymes with antimicrobial applications, *Recent Pat. Biotechnol. 1*, 113–122.
27. Fischetti, V. A. (2005) Bacteriophage lytic enzymes: novel anti-infectives, *Trends Microbiol. 13*, 491–496.
28. Jones, E. W. (1991) Tackling the protease problem in Saccharomyces cerevisiae, *Methods Enzymol. 194*, 428–453.
29. Wargo, M. J., Ho, T. C., Gross, M. J., Whittaker, L. A., and Hogan, D. A. (2009) GbdR regulates *Pseudomonas aeruginosa* plcH and pchP transcription in response to choline catabolites, *Infect. Immun. 77*, 1103–1111.
30. Knutson, C. A., and Jeanes, A. (1968) A new modification of the carbazole analysis: application to heteropolysaccharides, *Anal. Biochem. 24*, 470–481.
31. Herman, A., and Tawfik, D. S. (2007) Incorporating Synthetic Oligonucleotides via Gene Reassembly (ISOR): a Versatile Tool for Generating Targeted Libraries, *Protein Eng., Des. Sel. 20*, 219–226.
32. Krieger, E., Koraimann, G., and Vriend, G. (2002) Increasing the precision of comparative models with YASARA NOVA—a self-parameterizing force field, *Proteins 47*, 393–402.